ON THE SHAPE OF LIDAR RETURN IN PULSED SOUNDING A WAVY SEA SURFACE

M.L. Belov and B.M. Orlov

All–Union Scientific–Research Institute of Marine Fishing and Oceanography, Moscow

Received July 29, 1991

The shape of echo–signal is studied in pulsed laser sounding a sea surface. The expressions for the delay, width, and average power of echo–signal recorded by the lidar receiver in monostatic and bistatic sounding of a wavy foam–free sea surface and of a sea surface partially covered with foam are derived. It is shown that the configuration of lidar, its parameters, and foam formations substantially affect the shape of the echo–pulse being received.

Laser pulsed sounding is one of the promising methods of sounding of the state of the sea surface. The methods of pulsed sounding are based on measurements of the time delay between a sounding pulse and that reflected from the sea surface as well as measurements of the shape and width of reflected pulses.

The variances of heights and slopes are the most important statistical characteristics of the sea surface. These characteristics can be measured from onboard an aircraft, helicopter or spacecraft in pulsed laser sounding. The variance of heights of the irregularities can be found from broadening or slope of the leading edge of the short laser pulse reflected from the sea surface and the variance of slopes can be found from the increase in the width of the trailing edge of the reflected pulse (see, for example, Refs. 1–5). The average sea level can be evaluated the average time delay of echo–signals (see, for example, Ref. 4).

Laser methods, being indirect methods of measurements, do not give directly the characteristics of the sea surface. The values of these characteristics are related in a complicated way with the parameters of the received signal. The lidar configuration, the parameters of the receiver and transmitter of the lidar, the driving wind velocity, and the presence of foam on the sea surface are the most important factors determining the lidar return.

1. LIDAR RETURN IN SOUNDING THE FOAM–FREE SEA SURFACE

Let us first consider, sounding the sea surface for low driving wind velocity when scattering by foam formations can be ignored.

We assume that:

– heights and slopes of the sea surface obey the normal distribution;

– the wavelength of sounding radiation lies in the IR range, in which the absorption by water is high, so that the main contribution to the echo–signal comes from the light specularly reflected from the air–sea interface, and the contribution of radiation diffusely reflected from the water depth can be ignored;

– the wavelength of radiation is small compared with characteristic radii of curvature and the heights of irregularities of the sea surface;

– the change in the sea surface configuration during its interaction with the light pulse can be ignored; and,

– the sounding pulse width is large compared with the period of the carrier frequency.

Attempts to derive the general analytic formula for the average (over the ensemble of randomly rough surfaces) power of the echo–signal under these conditions result in very cumbersome expressions. Therefore, below the echo–signal is modeled for two most important cases: vertical sounding when the transmitter and receiver are collocated and sounding along the slant paths.

In vertical sounding, when the source and receiver are collocated, assuming that the heights and slopes of the sea surface obey the normal distribution, we have for the average power of the echo signal $P_\mathrm{s}(t)$ received from the sea surface under the above–enumerated conditions[5]

$$P_\mathrm{s}(t)=\frac{a_\mathrm{t}a_\mathrm{r}V^2}{4L^4}\frac{\pi}{\frac{1}{a^2}+l_\mathrm{r}}\frac{1}{\sqrt{2\pi}\sigma\left(\overline{\gamma_x^2}\;\overline{\gamma_y^2}\right)^{1/2}}\left(\frac{1}{2\sigma^2}+\frac{16}{\tau_\mathrm{t}^2c^2}\right)^{-1/2}\exp\left\{\frac{1}{8}y^2z-\frac{4(t')^2}{\tau_\mathrm{t}^2+\frac{32\sigma^2}{c^2}}\right\}\times\sum_{\mathrm{k}=0}^{\infty}\frac{1}{(\mathrm{k}!)^2}\left(\frac{b}{2}\right)^{2\mathrm{k}}\left(\frac{z}{2}\right)^{(2\mathrm{k}+1)/2}\times$$

$$\times\,\Gamma(2\mathrm{k}+1)\,D_{-2\mathrm{k}-1}\left(\frac{yz^{1/2}}{\sqrt{2}}\right), \qquad (1)$$

where

$$y=\frac{1}{2\overline{\gamma_x^2}\;L^2}+b+C_\mathrm{t}+C_\mathrm{r}-\frac{t'}{\frac{\tau_\mathrm{t}^2cL}{8}+\frac{4\sigma^2L}{c}}\;;\quad z=\frac{\tau_\mathrm{t}^2c^2L^2}{4}+8\sigma^2L^2\;;\; t'=t-\frac{2L}{c}\;;\; b=\frac{1}{2L^2}\left(\frac{1}{2\overline{\gamma_y^2}}-\frac{1}{2\overline{\gamma_x^2}}\right);\quad \alpha_\mathrm{t}=\frac{k^2P_0}{4\pi\mathrm{x}}\;;$$

$$a_\mathrm{r}=\frac{k^2r_\mathrm{r}^2}{4F^2\eta}\;;\; l_\mathrm{r}=\frac{k^2}{4F^2\eta}\;;\; C_\mathrm{r}=\frac{k^2}{4\zeta L^2};\; C_\mathrm{t}=\frac{k^2}{4\xi L^2}\;;\; \eta=\frac{1}{4r_\mathrm{r}^2}+\frac{k^2r_\mathrm{r}^2}{4L^2}\left(1-\frac{L\Delta}{F^2}\right)^2\;;\; \zeta=F+\frac{k^2a^2}{4F^2}\;;\; \xi=\frac{1}{4r_\mathrm{t}^2}+\frac{k^2r_\mathrm{t}^2}{4L^2}\left(1-\frac{L}{F_\mathrm{t}}\right)^2\;;$$

$\Gamma(K)$ is the gamma function, $D_k(x)$ is the parabolic cylinder function, F is the focal length of the receiving lens, Δ is the displacement of the photodetector plane with respect to the focal plane, P_0 is the transmitted power, F_t is the curvature of the phase front at the aperture of the laser transmitter, σ and $\overline{\gamma^2_{xy}}$ are the variances of heights and slopes of the randomly rough surface S, a is the effective size of the photodetector, r_r and r_t are the effective radii of the receiving and transmitting apertures, L is the distance from the center of the observation sector lying on the sea surface to the lidar, k is the wave number, and V^2 is the Fresnel reflectance. We assume the refractive index of water n to be constant over the illuminated shot on the sea surface, so that $V^2 = \left(\frac{n-1}{n+1}\right)^2$.

In the derivation of Eq. (1) we assumed the Gaussian shape of the sounding pulse and the Gaussian approximations for the directional patterns of the transmitter and receiver.[6]

In the case in which the field–of–view angle of the receiver is much larger than the angular divergence of the laser transmitter and sea waves are isotropic ($b = 0$), formula (1) agrees well with the results given in Ref. 4.

Taking even the first term in Eq. (1) into account, we can obtain a good approximation for the slightly anisotropic sea waves.

In bistatic sounding along the slant paths, when the transmitter and receiver are separated, we have for the average power of the echo–signal (assuming shading of some sea surface elements by others to be negligible)[5]

$$P_s(t) \simeq \frac{q^4}{q_z^4}\,\frac{V^2 a_t a_r \pi K_T \bar{\nu}^{-1/2}\,\omega^{-1/2}}{4L_t^2 L_r^2 (a^{-2} + l_r)\,\sigma\sqrt{2\pi}\,(\overline{\gamma_x^2}\;\overline{\gamma_y^2})^{1/2}}\left[C_t + C_r + \frac{k^2}{2\overline{\gamma_y^2}\,g_z^2}\left(\frac{1}{L_t}+\frac{1}{L_r}\right)^2\right]^{-1/2} \exp\Bigg\{-\frac{q_x^2}{2\overline{\gamma_x^2}\,q_z^2} - \frac{4(t')^2}{\tau_t^2} +$$

$$+\frac{1}{\bar{\nu}}\left[-\frac{q_x\,\kappa}{2\overline{\gamma_x^2}\;\overline{q_z^2}}\left(\frac{\cos^2\theta_t}{L_t}+\frac{\cos^2\theta_r}{L_r}\right)+\frac{4t'}{\tau_t^2 c}(\sin\theta_t+\sin\theta_r)\right]^2 + \frac{1}{\omega}\Bigg[\frac{\kappa}{\bar{\nu}}\left(\frac{q_x k}{2\overline{\gamma_x^2}\;\overline{q_z^2}}\left(\frac{\cos^2\theta_t}{L_t}+\frac{\cos^2\theta_r}{L_r}\right)-\frac{4t'}{\tau_t^2 c^2}(\sin\theta_t+\sin\theta_r)\right) -$$

$$-\frac{4t'}{\tau_t^2 c}(\cos\theta_t+\cos\theta_r)\Bigg]^2\Bigg\}, \tag{2}$$

where

$$\omega = \frac{1}{2\sigma^2} + C_t\sin^2\theta_t + C_r\sin^2\theta_r + \frac{4}{\tau_t^2 c^2}(\cos\theta_t+\cos\theta_r)^2 - \frac{\kappa}{\bar{\nu}};$$

$$\kappa = C_t\sin\theta_t\cos\theta_t + C_r\sin\theta_r\cos\theta_r - \frac{4}{\tau_t^2 c^2}(\sin\theta_t+\sin\theta_r)(\cos\theta_t+\cos\theta_r);$$

$$\bar{\nu} = \frac{k^2}{2\overline{\gamma_x^2}q_z^2}\left(\frac{\cos^2\theta_t}{L_t}+\frac{\cos^2\theta_r}{L_r}\right)^2 + C_t\cos^2\theta_t + C_r\cos^2\theta_r + \frac{4}{\tau_t^2 c^2}(\sin\theta_t+\sin\theta_r)^2;\ q_x = k(\sin\theta_t+\sin\theta_r);\ q_z = -k(\cos\theta_t+\cos\theta_r);\ q^2 = q_z^2 + q_x^2;$$

$$K_T = 1 - \mathrm{L}\left(\frac{\mathrm{cotan}^2\alpha}{\overline{\gamma^2}}\right);\ |\alpha| = \max(|\theta_t|, |\theta_r|),\ \text{for } \theta_t, \theta_r > 0;\ \theta_t, \theta_r < 0;\ K_T = \left[1 - \Lambda\left(\frac{\mathrm{cotan}^2\theta_t}{\overline{\gamma^2}}\right)\right]\left[1 - \Lambda\left(\frac{\mathrm{cotan}^2\theta_r}{\overline{\gamma^2}}\right)\right];$$

$$\text{for } \theta_t > 0,\ \theta_r < 0;\ \theta_t < 0,\ \theta_r > 0;\ \Lambda(a) = \frac{1}{\sqrt{2\pi}\,a^{3/2}}\exp\left(-\frac{a}{2}\right);$$

θ_t and θ_r are the angle of radiation incident on the surface and the observation angle, respectively (they are counted off from the normal to the underlying surface); L_t and L_r are the distances from the center of the observation sector to the transmitter and receiver.

We assume in Eq. (2) that θ_t and θ_r differ slightly, so that $V^2(\theta) \approx V^2$ (θ is the local angle of radiation incident on the sea surface).

In the limiting case as σ^2, $\overline{\gamma^2_{xy}} \to 0$, Eq. (2) transforms into the expression for the power received from the flat specular surface.

In monostatic sounding (the transmitter and receiver are collocated, $L_t = L_r = L$ and $\theta_t = \theta_r = \theta$) we have for the delay and width of the echo signal[7] (for $\sigma^2 \ll (C_t + C_r)^{-1}$ and $L^2\overline{\gamma_x^2}$)

$$T_s \simeq \frac{2L}{c} - \frac{2L}{c}\tan^2\theta\,\frac{\frac{1}{2\sigma^2} + C_t + C_r}{\frac{1}{2\sigma^2} + (C_t + C_r)\sin^2\theta + L^2 2\overline{\gamma_x^2}\,\frac{(C_t + C_r)}{2\sigma^2}} + \frac{1}{2cL}\left\{\left[\left(L^2\cos^2\theta\,2\overline{\gamma_y^2}\right)^{-1} + C_t + C_r\right]^{-1} + \bar{p}^{-1}\right\} + \frac{\sin^2\theta\,\bar{p}^{-2}}{L^2\,(2\overline{\gamma_x^2})^2 cL};\tag{3}$$

$$\tau_s^2 \simeq \frac{\tau_t^2}{8} + \frac{4\sigma^2\alpha}{c^2\cos^2\theta} + \frac{2\sin^2\theta\alpha}{c^2\cos^2\theta\,(C_t + C_r)} + \frac{4\sigma^2\alpha\cos^2\theta}{c^2 L^2 2\overline{\gamma_x^2}(C_t + C_r)} + \frac{1}{2c^2 L^2}\left[\left(\frac{1}{L^2 2\overline{\gamma_y^2}\cos^2\theta} + C_t + C_r\right)^{-2} + \right.$$

$$\left. + \left(\frac{1}{L^2 2\overline{\gamma_x^2}} + C_t + C_r\right)^{-2}\cos^4\theta\right] - \frac{4\sin^2\theta}{\cos^4\theta}\,\frac{1}{c^2L^2}\,\frac{\alpha^2}{2\overline{\gamma_x^2}(C_t + C_r)^2} - \left[1 - \frac{(1 + 2L^2\overline{\gamma_x^2}\,(C_t + C_r))^{-1}}{2\cos^2\theta}\right]; \qquad (4)$$

where

$$\overline{p} = \cos^2\theta\,(L^2 2\overline{\gamma_x^2})^{-1} + (C_t + C_r)\cos^2\theta\,(1 + 2\sigma^2\,(C_t + C_r)\sin^2\theta)^{-1}\,;\ \alpha = \left[1 + (L^2 2\overline{\gamma_x^2}(C_t + C_r))^{-1}\right]^{-1}.$$

Formulas (3) and (4) are valid for both vertical and slant monostatic sounding.

For sounding in the nadir direction, when the sea waves are isotropic ($\overline{\gamma_x^2} = \overline{\gamma_y^2} = \overline{\gamma^2}$) and the angular divergence of laser transmitter is much smaller than the field–of–view angle of the receiver ($C_r \ll C_t$) Eqs. (3) and (4) agree well with the results given in Ref. 4.

As follows from Eq. (4), the width of the received signal depends on the rms value of the sea surface slopes. Figure 1, which shows the dependence of $\dfrac{\tau_s^2}{\tau_s^2\,(x = 0)}$ on the parameter $x = \dfrac{\alpha_t^2}{2\,\overline{\gamma_x^2}}$, can be used to determine the domain in which this effect is important. Calculations were performed with the following values of the parameters: $C_t^{-1/2} = 10^2$ m, $\sigma = 1$ m, $\tau_t = 10^{-8}$ s, and $\alpha_r \gg \alpha_t$. Curve *1* is for $\theta = 10^\circ$, curve *2* is for $\theta = 40^\circ$, and curve *3* is for $\theta = 60^\circ$.

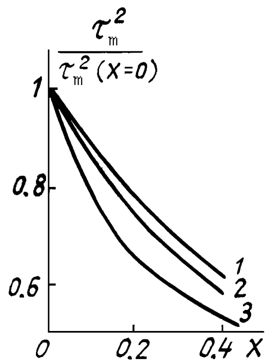

FIG. 1 Echo–signal width for the case of sounding the sea surface without foam.

The width of the received signal substantially decreases in the domain in which the rms value of sea surface slopes becomes comparable with the angular divergence of laser transmitter (in the domain in which x is noticeably different from zero).

2. LIDAR RETURN IN SOUNDING THE SEA SURFACE COVERED WITH FOAM

The sea surface is covered with foam at high wind velocities. To take radiation reflected from the sea surface into account, it is necessary to know the relative fraction of the surface covered with foam as a function of the wind velocity and reflection characteristics of foam.

Covering of the ocean surface with foam has been studied in a number of works in which the empirical relations for the relative fraction of the sea surface covered with foam and whitecaps have been derived. In Ref. 8 the results of investigation of the sea surface state have been analyzed and the statistical dependences of the relative fraction of the sea surface covered with whitecaps S_w and foam S_f on the wind velocity have been refined.

We assume that sections of foam lie on the slopes of the waves and are Lambertian reflectors.[8-12]

The model of the echo–signal being received from the sea surface partially covered with foam because of the fact that the echo–signals received from the sections of foam–free and foam–covered sea surfaces are added together incoherently, can be represented in the form

$$P(t) = (1 - S_0)\,P_s(t) + S_0\,P_f(t)\,, \qquad (5)$$

where $P(t)$, $P_s(t)$, and $P_f(t)$ are the average powers received by the lidar when sounding the sea surface partially covered with foam, foam–free, and continuously covered with foam, respectively; $S_0 = S_f = S_w$.

We will use two models of the sea surface continuously covered with foam: the model of the flat Lambertian surface and the model of the randomly rough locally Lambertian surface whose distribution of slopes is the same as the distribution of the wave slopes.[11,12]

Below the echo–signals are modeled for two most important cases: vertical sounding, when the transmitter and receiver are collocated and sounding along the slant paths. We consider that all assumptions enumerated in Section 1 are valid.

When the sea surface covered with foam is vertically sounded, the transmitter and receiver are collocated, and the sea waves are slightly anisotropic, we derive the following expression for the average power of the echo–signal[13,14]:

$$P(t) = C_1\left\{C_2\exp\left\{\frac{N_0^2\,z}{4} - t'N_0Lc\right\}\right. \times$$

$$\times\left\{1 - \Phi\left[\frac{N_0\,z^{1/2}}{2} - t'\,\frac{cL}{z^{1/2}}\right]\right\} + C_3\exp\left\{\frac{N_r^2\,\tilde{z}}{4} - t'N_0\,Lc\right\}\times$$

$$\left.\times\left\{1 - \Phi\left[\frac{N_r\,\tilde{z}^{1/2}}{2} - t'\,\frac{cL}{\tilde{z}^{1/2}}\right]\right\}\right\}, \qquad (6)$$

where

$C_1 = \dfrac{a_t a_r}{L^4}\dfrac{\tau_t c L}{2}$; $C_2 = (1 - S_o)\dfrac{V^2}{8\pi}(\overline{\gamma_x^2}\,\overline{\gamma_y^2})^{-1/2}$; $\Phi(x)$ is the Fresnel integral;

$N_r = C_t + C_r$; $N_0 = N_r + (4\overline{\gamma_x^2}\,L^2)^{-1} + (4\overline{\gamma_y^2}\,L^2)^{-1}$.

For the model of a randomly rough locally Lambertian surface,[13,14] we have $C_3 = \dfrac{1}{\pi}S_0 A Q_B$ and $\tilde{z} = z$, where Q_B is the function depending on $\overline{\gamma_{xy}^2}$ (Refs. 13 and 14).

For the model of a flat Lambertian surface, we have $C_3 = \dfrac{1}{\pi}S_0 A$ and $\tilde{z} = z(\sigma = 0)$.

Figures 2 and 3 show the calculational results of the shape of the echo pulse received from the sea surface for various velocities of the driving wind U. The values of $\dfrac{P(t)}{C_1 \cdot C_2}$ were calculated for the models of a randomly rough locally Lambertian surface (solid curves) and of a flat Lambertian surface (dashed curves) with the following values of the parameters: $L = 10$ km; $\alpha_r = 2.9\cdot10^{-2}$; $\tau_t = 10^{-8}$ s and $\alpha_t = 8.7\cdot10^{-3}$ (Fig. 2); $\tau_t = 10^{-9}$ s and $\alpha_t = 10^{-3}$ (Fig. 3); $U = 2$ (curve *1*) and 14 m/s (curve *2*) (Fig. 2); and, $U = 14$ m/s (Fig. 3).

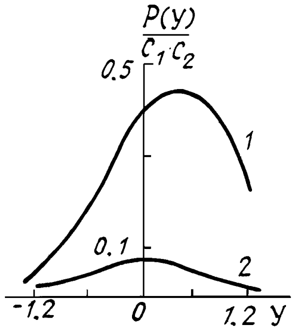

FIG. 2. Echo–signal shape for the vertical sounding when $\tau_t = 10^{-8}$ s *and* $\alpha_t = 8.7\cdot10^{-3}$.

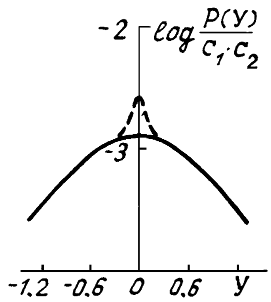

FIG. 3. Echo–signal shape for the vertical sounding when $\tau_t = 10^{-9}$ s *and* $\alpha_t = 10^{-3}$.

Hereafter the values $\overline{\gamma_x^2}$ and $\overline{\gamma_y^2}$ were calculated using the Cox–Munk formulas,[15] and the quantities S_o and σ were calculated from the following expressions[4,8]:

$S_0 = 0.009\,U^3 - 0.3296\,U^2 + 4.549\,U - 21.33$; $\sigma = 0.016\,U^2$.

It can be seen from the figures that the presence of foam on the sea surface for the high wind velocity affects the amplitude and the shape of the echo–pulse. For the laser beam with $\alpha_t = 8.7\cdot10^{-3}$ the echo–pulse amplitude depends weakly on the model of foam (solid and dashed curves are superimposed in Fig. 2). For sufficiently narrow laser beam with $\alpha_t = 10^{-3}$, the echo–pulse shape depends strongly on the model of foam (see Fig. 3).

For bistatic slant sounding the sea surface covered with foam for the average power of the echo–signal (assuming the shading of some surface elements by the others to be negligible), we have[16]

$$P(t) = b_1 K_T \{b_2 \exp[-\hat{z}^2 - \hat{z}\bar{d}] + b_3 \exp[-\hat{z}^2 R]\} , \quad (7)$$

where

$$b_1 = \frac{a_t a_r}{L_t^2 L_r^2} N_r^{-1/2} \frac{2}{\sqrt{\pi}} \bar{\nu}^{-1/2}\bar{\omega}^{-1/2} \; ; \; \bar{\omega} = 2\sigma^2\omega \; ;$$

$$b_2 = (1 - S_o)\frac{q^4}{q_z^4}\frac{V^2}{8\,(\overline{\gamma_x^2}\,\overline{\gamma_y^2})^{1/2}} \exp\left\{ - \frac{q_x^2}{q_z^2 2\overline{\gamma_x^2}} \right\} ;$$

$\hat{z} = t'\sqrt{\alpha}$; $\alpha = \dfrac{1}{2}(\tau_s^2)^{-1}$; $\mu = \sin\theta_t + \sin\theta_r$; $\nu = \cos\theta_t + \cos\theta_r$;

$$\bar{d} = \frac{\alpha^{-1/2}8}{\tau_t^2\, c\bar{\nu}}\left[\mu + \frac{k}{\omega\bar{\nu}}(\mu k + \nu\bar{\nu})\right]\frac{kq_x}{q_z^2\, 2\overline{\gamma_x^2}}\left(\frac{\cos^2\theta_t}{L_t} + \frac{\cos^2\theta_r}{L_r}\right) .$$

For the model of the randomly rough locally Lambertian surface,[16] we have $b_3 = S_0 A Q$ and $R = 1$, where Q is the function of θ_t and θ_r $\overline{\gamma_{xy}^2}$ (Ref. 16).

For the model of a flat Lambertian surface, we have $b_3 = S_0 A\cos\theta_t \cos\theta_r\ \overline{\omega^{-1/2}}$, $R = \alpha_0/\alpha$, and $\alpha_0 = \alpha(\sigma = 0)$.

The second term in formula (7) (corresponding to the contribution of the sections of the foam–covered surface to the echo–signal) is the same (without terms K_t and S_0) as the expression for the echo–signal received from flat[6,17] or randomly rough[18] Lambertian surfaces.

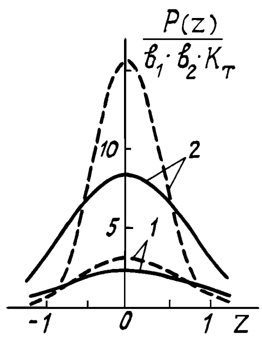

FIG. 4. Echo–signal shape for the case of slant sounding.

Figure 4 shows the results of calculation of the echo–signal shape received from the sea surface covered with foam for different velocities of the driving wind U when sounding along the slant paths. Calculations were performed for the model of a randomly rough locally Lambertian surface (solid curves) and of a flat Lambertian surface (dashed curves) with the following values of the parameters: $\theta_t = \theta_r = 30^\circ$, $L_t = L_r = 10$ km, $\alpha_r = 2.9\cdot10^{-2}$, $\tau_t = 10^{-10}$ s, $\alpha_t = 10^{-3}$, and $U = 14$ (curve *1*) and 18 m/s (curve *2*).

It can be seen from the figure that not only the presence of foam but also the model of foam used in calculations affects the amplitude and shape of the echo–signal when sounding along the slant paths. The model of foam affects strongly only for narrow laser beams when the illuminated spot size on the surface being sounded becomes comparable with the height of irregularities.

In the case of lidar sounding the surface covered with foam the echo–pulse delay T and its width τ^2 are determined by the formulas[13,14,16]

$$T = T_s K_s + T_f K_f \; ; \tag{8}$$

$$\tau^2 = \tau_s^2 K_s + \tau_f^2 K_f \; , \tag{9}$$

where T_s,τ_s and T_f,τ_f are the delays and widths of the echo–pulses in sounding the foam–free sea surface and the surface continuously covered with foam.

In the particular case of sounding in the nadir direction we have

$$K_s = \frac{1}{1 + a_0} \; ; \; K_f = \frac{a_0}{1 + a_0} \; ;$$

For the model of a randomly rough locally Lambertian surface,[13,14] we have

$$a_0 = \frac{A Q_B S_0 \, 8(\overline{\gamma_x^2} \; \overline{\gamma_y^2})^{1/2}}{(1 - S_0)\, V^2} \frac{(a_1 a_2)^{1/2}}{N_r} \; ; \; \alpha_{1,2} = N_r + \frac{1}{2\gamma_{x,y}^2 L^2} \; ;$$

$$T_f = \frac{2L}{c} + \frac{1}{Lc(C_t + C_r)} \; , \tag{10}$$

$$\tau_f^2 = \frac{\tau_r^2}{8} + \frac{4\sigma^2}{c^2} + [(C_t + C_r)Lc]^{-2} \; . \tag{11}$$

For the model of a flat Lambertian surface we have

$$a_0 = \frac{A S_0 8(\overline{\gamma_x^2} \; \overline{\gamma_y^2})^{1/2}}{(1 - S_0) V^2} \frac{(a_1 a_2)^{1/2}}{N_r} \; ,$$

T_f and τ are given by formulas (10) and (11) for $\sigma = 0$.

The quantities T_s and τ are given by formulas (3) and (4) for the case of vertical sounding.

Figure 5 shows the results of calculation of the width of the echo–signal received from the sea surface for various driving wind velocity. Calculations of τ^2 were performed for the model of a randomly rough locally Lambertian surface (solid lines) and of a flat Lambertian surface (dashed lines) with the following values of the parameters: $L = 10$ km, $\alpha_r = 2.9\cdot10^{-2}$, $\alpha_t = 10^{-3}$, and $\tau_t = 10^{-9}$ s.

It can be seen from the figure that the echo–pulse width depends on both the driving wind velocity and the employed model of foam. However, the latter dependence is manifested only for high driving wind velocity alove.

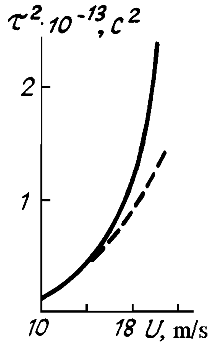

FIG. 5. Echo–signal width for the case of sounding the sea surface partially covered with foam.

Generalizing the results of the investigations, we can draw the following conclusions[5,7,13,14,16]:

a) the shape of lidar return received from the sea surface depends strongly on the lidar configuration (monostatic or bistatic sounding and sounding in the nadir direction or along the slant paths), the relation of the parameters of radiation of a lidar (angular divergence and the spot size of radiation on the sea surface), and statistical characteristics of the wind–driven sea waves (rms values of slopes and heights of irregularities of the sea surface);

b) the presence of foam on the sea surface affects strongly the echo–signal amplitude for all operating conditions of a sounding system (monostatic or bistatic sounding and sounding in the nadir direction or along the slant paths);

c) the effect of the model of foam on the echo–signal is manifested, as a rule, only for the high driving wind velocity and sufficiently narrow laser beams (when the illuminated spot size on the surface being sounded becomes comparable with the rms height of irregularities); and,

d) the effect of the atmosphere on the echo–signal depends in a complicated way on the operating condition of the sounding system and on the model of foam. Atmospheric turbidity sharply reduces the effect of foam on the echo–signal shape for pulsed sounding.

In conclusion we note that the same investigations of the average power recorded by the receiver for the case of continuous exposure and of the average illumination in the image plane of the lidar receiver, when sounding the foam–free sea surface and that covered with foam, were carried out in Refs. 19–22.

REFERENCES

1. G.S. Gurevich, in: *Abstracts of Reports at the 4th All–Union Symposium on Laser and Acoustic Sounding of the Atmosphere,* Tomsk (1976), 127 pp.

2. A.I. Stemkovskii, *"Measurements of the parameters of sea waves by laser radar techniques"*, Author's Abstract Cand. Phys.–Math. Sci. Diss., Institute of Oceanography of the Academy of Sciences of the USSR (1984), 16 pp.

3. V.N. Pelevin, in: *Light Fields in the Ocean* (State Oceanographic Institute Publishing House, Moscow, 1980), 216–223 pp.

4. B.M. Tsai and C.S. Gardner, Appl. Opt. **21**, No. 21, 3932–3940 (1982).

5. M.L. Belov, *"Remote Sounding of a Sea Surface. Part 1. Pulsed Laser Detection and Ranging,"* BNIERKH, No. 1018–px 89, Moscow, March 29, 1989, 24 pp.

6. V.M. Orlov, I.V. Samokhvalov, G.G. Matvienko, et al., *Elements of Light Scattering Theory and Optical*

Detection and Ranging (Nauka, Novosibirsk, 1982), 225 pp.
7. M.L. Belov, V.M. Orlov, and R.G. Safin, Opt. Atm. **1**, No. 10, 106–108 (1988).
8. R.S. Bortkovskii, Meteorol. Gidrol., No 5, 68–75 (1987).
9. P. Koepke, Int. J. Remote Sensing **6**, No. 5, 787–799 (1985).
10 P. Koepke, Appl. Opt. **23**, No. 11, 1816–1824 (1984).
11. O.V. Kopelevich and E.M. Mezhericher, Okeanologiya **20**, No. 1 50–56 (1980).
12. L. Wald and J.M. Monget, Int. J. Remote Sensing **4**, No. 2, 433–446 (1988).
13. M.L. Belov and V.M. Orlov, Atm. Opt. **3**, No. 7, 677–681 (1990).
14. V.M.Orlov, M.L. Belov, and V.A. Balyakin, in: *Abstracts of Reports of the 15th International* Laser Radar Conference, Tomsk (1990), 44–48 pp.
15. C. Cox and W. Munk, J. Opt. Soc. Amer. **44**, No. 11, 839–850 (1954).
16. M.L. Belov and V.M. Orlov, Atm. Opt. **4**, No. 4, 317–321 (1991).
17. V.M. Orlov, I.V. Samokhvalov, G.M. Krekov, et al., *Signals and Noise in Laser Detection and Ranging* (Radio i Svyaz', Moscow, 1985), 264 pp.
18. M.L. Belov, V.M. Orlov, and I.V. Samokhvalov, Opt. Spectrosk. **64**, No. 4, 937–939 (1988).
19. M.L. Belov and V.M. Orlov, Atm. Opt. **3**, No. 4, 387–391 (1990).
20. M.L. Belov and V.M. Orlov, Atm. Opt. **2**, No. 7, 641–644 (1989).
21. M.L. Belov, V.M. Orlov, and I.V. Samokhvalov, Atm. Opt. **2**, No. 2, 173–172 (1989).
22. M.L. Belov and V.M. Orlov, Atm. Opt. **2**, No. 10, 945–948 (1989).